

# A NOTE ON AN EXTENDED CLARIFIER-THICKENER MODEL WITH SINGULAR SOURCE AND SINK TERMS

R. BÜRGER<sup>A</sup>, A. GARCÍA<sup>A</sup>, K.H. KARLSEN<sup>B</sup>, AND J.D. TOWERS<sup>C</sup>

**ABSTRACT.** A one-dimensional clarifier-thickener (CT) model, which includes a singular feed source, can be expressed as a conservation law with a flux that is discontinuous with respect to the spatial variable. The CT model is extended herein by a singular sink through which material is extracted. The sink gives rise to a new non-conservative transport term. The paper summarizes a recent well-posedness analysis and presents a numerical method for the extended model. A numerical example is presented.

## 1. INTRODUCTION

In recent years there has been an increased interest in conservation laws with a discontinuous flux of the type  $u_t + f(\gamma(x), u)_x = 0$  where  $x \in \mathbb{R}$ ,  $t > 0$ , and  $\gamma(x)$  is a vector of parameters that are discontinuous functions of the spatial position  $x$ . Applications of this equation include two-phase flow in heterogeneous porous media, traffic flow, and CT models [3]. Its well-posedness and numerical analysis is not a straightforward limit case of the standard theory for conservation laws with a flux that depends smoothly on  $x$ . In fact, several extensions of the Kružkov [13] entropy solution concept to a flux that depends discontinuously on  $x$  have been proposed [1, 2, 10, 12, 14, 15, 16]. For CT models, the entropy solution emerges from the limit  $\varepsilon \rightarrow 0$  of a viscous regularization  $\varepsilon u_{xx}$  with a diffusion constant  $\varepsilon > 0$  [6, 7].

CT units are widely used in engineering for the solid-liquid separation of suspensions. Important contributions to their analysis were made by Diehl, see [8] and references. On the other hand, in [4, 5, 6] the authors with collaborators provided a rigorous well-posedness and numerical analysis for CT models. Their basic non-standard ingredient is a singular feed source that produces diverging bulk flows in the unit, and generates the discontinuous  $x$ -dependence of the flux. We herein present a new extended clarifier-thickener (ECT) model that also includes a singular sink term, through which material may be extracted, and show that the new model is well posed and can be simulated by a convergent numerical scheme.

---

*Date:* May 30, 2006.

*Key words and phrases.* Conservation law, discontinuous flux, source term, sink term, entropy solution, jump condition, numerical method.

<sup>A</sup>Departamento de Ingeniería Matemática, Facultad de Ciencias Físicas y Matemáticas, Universidad de Concepción, Casilla 160, Concepción, Chile. E-Mail: [rburger@ing-mat.udec.cl](mailto:rburger@ing-mat.udec.cl), [agarcia@ing-mat.udec.cl](mailto:agarcia@ing-mat.udec.cl). RB acknowledges support by Fondecyt project 1050728 and Fondap in Applied Mathematics. AG acknowledges support by MECESUP project UCO0406.

<sup>B</sup>Centre of Mathematics for Applications (CMA), University of Oslo, P.O. Box 1053, Blindern, N-0316 Oslo, Norway. E-Mail: [kennethk@math.uio.no](mailto:kennethk@math.uio.no). The research of KHK is supported by an Outstanding Young Investigators Award (OYIA) from the Research Council of Norway.

<sup>C</sup>MiraCosta College, 3333 Manchester Avenue, Cardiff-by-the-Sea, CA 92007-1516, USA. E-mail: [john.towers@cox.net](mailto:john.towers@cox.net).

The basic CT model can be derived from the scalar conservation law  $u_t + b(u)_x = 0$ ,  $x \in [0, L]$ ,  $t > 0$  of the kinematic sedimentation model, which describes the settling of a suspension in a column of height  $L$ . Here,  $u \in [0, u_{\max}]$  is the sought concentration as a function of depth  $x$  and time  $t$ , and  $b(u)$  is the material-dependent hindered settling or batch flux density function. A typical example is

$$(1) \quad b(u) = v_{\infty} \chi_{[0, u_{\max}]}(u) u(1 - u)^n, \quad n > 1, \quad v_{\infty} > 0,$$

where  $v_{\infty}$  is the settling velocity of a single particle in an unbounded medium.

Suppose now that we pump the suspension into a vertical tube that is filled with water at a feed level  $x = 0$  at volume rate  $Q_F$ , and that part of the mixture flows upwards (i.e., in the direction of negative  $x$ ) at velocity  $q_L < 0$ , while the remainder flows downwards at velocity  $q_R > 0$ . Consequently, if  $\mathcal{S}$  is the cross-sectional area, then  $Q_F = (q_R - q_L)\mathcal{S}$ . Now if we inject feed suspension of concentration  $u_F$  at a volume rate  $Q_F$ , then the governing conservation law can be written as

$$(2) \quad u_t + g(u, x)_x = 0, \quad g(u, x) := \begin{cases} q_L(u - u_F) + b(u) & \text{for } x < 0, \\ q_R(u - u_F) + b(u) & \text{for } x \geq 0. \end{cases}$$

Note that the *injection* of material leads to a homogeneous conservation law with discontinuous flux, which has made the CT problem tractable.

We herein study the case that we also extract material at a fixed location. To elucidate the problem, consider a column with an upwards directed bulk flow of  $Q_R < 0$ . At depth  $x = 0$ , we divide the flow into a discharge flow  $Q_D < 0$  and the remaining upwards directed bulk flow  $Q_L$  with  $Q_R < Q_L < 0$ . Considering that the concentration  $u(0, t)$  of the suspension extracted is unknown beforehand and defining  $q_R := Q_R/\mathcal{S}$  and  $q_L := Q_L/\mathcal{S}$ , we obtain instead of (2) the equation

$$(3) \quad u_t + h(u, x)_x = \delta(x)(q_R - q_L)u(x, t), \quad h(u, x) = \begin{cases} q_L u + b(u) & \text{for } x < 0, \\ q_R u + b(u) & \text{for } x > 0. \end{cases}$$

The singular sink term on the right-hand side of (3) includes the *unknown* solution value  $u(x, t)$ , while the analogous term for the singular injection source involves the *given* constant  $u_F$ . This difference makes the sink term problem interesting.

Equation (3), which includes a new sink term, after slight notational simplification, forms the so-called *reduced problem* studied in our paper. This is opposed to the *full ECT model* which also includes singular source terms and flux discontinuities; however, from [5] we already know how to deal with the latter ingredients.

The remainder of this note is organized as follows. The ECT model is outlined in Section 2. The result is a conservation law with a flux that is discontinuous at the source and transition points (not at the sink point), and which has a non-conservative linear flux term. Furthermore, we derive the reduced problem that includes the singularities caused by the new sink term only. This problem is analyzed further on in Section 3. We first define entropy solutions for the reduced problem. We then prove by an adaptation of the “doubling of variables” argument [13] an  $L^1$  stability property, and therefore uniqueness, of an entropy solution. In Section 4, we introduce a finite difference scheme for the complete model. We prove that the numerical solution remains bounded, that the scheme is monotone, and that it satisfies a time continuity property. In Section 5 we focus on the reduced

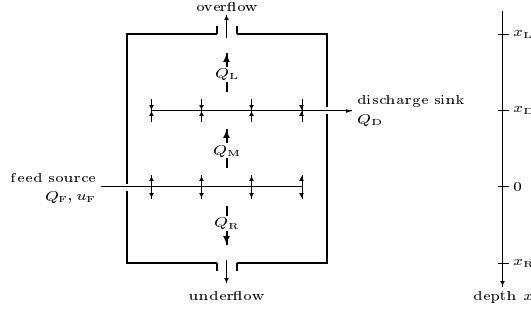


FIGURE 1. ECT setup with bulk flows and control variables.

problem, prove a discrete spatial variation bound, and show that the scheme converges to an entropy solution. Combining the new results with those of [5] yields that the full ECT model is well-posed. Section 6 presents a numerical example.

## 2. THE EXTENDED CLARIFIER-THICKENER MODEL

**2.1. Bulk flow variables.** Consider the ECT drawn in Figure 1. At  $x = 0$ , suspension is fed into the unit at a volume rate  $Q_F(t) \geq 0$ . The feed suspension is loaded with solids of the volume fraction  $u_F(t) \in [0, u_{\max}]$ , and  $u_{\max}$  is a maximum solids concentration. At  $x = 0$ , the feed flow divides into an upwards-directed and a downwards-directed bulk flow. We assume that the underflow volume rate  $Q_R(t) \geq 0$  is also prescribed, and that  $Q_R(t) \leq Q_F(t)$ . Thus, the signed volume rate of the upwards-directed bulk flow immediately above the feed source is  $Q_M(t) = Q_R(t) - Q_F(t) \leq 0$ . At depth  $x = x_D$ ,  $x_L < x_D < 0$ , a discharge sink is located. Suspension is extracted at a signed volume rate  $Q_D(t) \leq 0$ , where  $Q_D(t) \geq Q_M(t)$ . Above the discharge sink, for  $x_L \leq x \leq x_D$ , there is an upwards directed bulk flow with the volume rate  $Q_L(t) = Q_M(t) - Q_D(t) = Q_R(t) - Q_F(t) - Q_D(t) \leq 0$ . We assume that all control variables are constant, and introduce the velocities  $q_c := Q_c/\mathcal{S}$ ,  $c \in \{D, F, L, M, R\}$ ,  $\tilde{q}_R := q_R - q_D$  and the discontinuous parameters

$$(4) \quad \begin{aligned} \gamma^1(x) &:= \begin{cases} 0 & \text{for } x \notin [x_L, x_R], \\ 1 & \text{for } x \in [x_L, x_R], \end{cases} & \gamma^2(x) &:= \begin{cases} \tilde{q}_R - q_F & \text{for } x < 0, \\ \tilde{q}_R & \text{for } x > 0, \end{cases} \\ \gamma^3(x) &:= \begin{cases} 0 & \text{for } x < x_D, \\ -q_D > 0 & \text{for } x > x_D, \end{cases} & \gamma(x) &:= (\gamma^1(x), \gamma^2(x)). \end{aligned}$$

Then the final governing balance law is (see [3] for details)

$$(5) \quad u_t + f(\gamma(x), u)_x = \gamma^3(x)u_x,$$

$$(6) \quad f(\gamma(x), u) := g(u, x) = \gamma^1(x)b(u) + \gamma^2(x)(u - u_F).$$

If we set the right side of (5) to zero, we have essentially the PDE analyzed in [5].

**2.2. Reduced problem.** The flux discontinuities at  $x_L$ , 0 and  $x_R$  are the same as in [5]. They can be incorporated once the discontinuity near  $x = x_D$  can be handled. Our analysis is therefore focused on the following reduced problem:

$$(7) \quad u_t + \varphi(u)_x - \gamma(x)u_x = 0, \quad x \in \mathbb{R}, \quad t > 0,$$

$$(8) \quad u(x, 0) = u_0(x), \quad x \in \mathbb{R}, \quad u_0 \in [0, u_{\max}],$$

$$(9) \quad \varphi(u) = qu + b(u), \quad \gamma(x) = \begin{cases} 0 =: \gamma_- & \text{for } x < 0, \\ \gamma_+ & \text{for } x > 0, \end{cases}$$

where the sink has been moved to  $x = 0$  and the velocities have been normalized such that  $q_D$  (in the original problem description) equals  $-\gamma_+$ , and that  $q \leq 0$ .

The function  $b(u)$  is assumed to be Lipschitz continuous, positive for  $u \in (0, 1)$ , and to vanish for  $u \notin (0, 1)$ . We assume that  $b(u)$  is twice differentiable in  $(0, 1)$ , that  $b'(u)$  vanishes at exactly one maximum  $u = u_b^* \in (0, 1)$ , and that  $b''(u)$  vanishes at no more than one inflection point in  $u_{\text{infl}} \in (0, 1)$ ; if such a point is present, we assume that  $u_{\text{infl}} \in (u_{\text{max}}, 1)$ . These assumptions are valid for (1) with  $u_{\text{max}} = 1$ . With these assumptions on  $b(u)$  and the sign of  $q$ , the flux  $\varphi(u) = b(u) + qu$  will have a single maximum located at the point  $u^* \in [0, 1]$ , and  $\varphi$  will be non-decreasing on  $[0, u^*]$  and non-increasing on  $[u^*, 1]$ . Note that we refer to (7)–(9) as *reduced problem*, while (4)–(5) and (8) form the *full ECT model*.

### 3. ENTROPY SOLUTION AND UNIQUENESS ANALYSIS OF THE REDUCED PROBLEM

**Definition 3.1** (Entropy solution). *A function  $u : \Pi_T \mapsto \mathbb{R}$  is an entropy solution of the initial value problem (7)–(9) if it satisfies the following conditions:*

(D.1)  $u \in L^1(\Pi_T) \cap BV(\Pi_T)$  and  $u(x, t) \in [0, 1]$  for a.e.  $(x, t) \in \Pi_T$ .

(D.2) If  $0 \leq \psi \in \mathcal{D}(\Pi_T)$  vanishes for  $x > 0$ , then

$$(10) \quad \iint_{\Pi_T} (|u - c| \psi_t + \text{sgn}(u - c)(\varphi(u) - \varphi(c))\psi_x) dt dx \geq 0 \quad \forall c \in \mathbb{R},$$

and if  $0 \leq \psi \in \mathcal{D}(\Pi_T)$  vanishes for  $x < 0$ , then

$$(11) \quad \iint_{\Pi_T} (|u - c| \psi_t + \text{sgn}(u - c)(\varphi(u) - \varphi(c) - \gamma_+(u - c))\psi_x) dt dx \geq 0 \quad \forall c \in \mathbb{R}.$$

(D.3) With the abbreviation  $u_{\pm} = u(0 \pm, t)$ , the following jump conditions hold at  $x = 0$  for a.e.  $t \in (0, T)$ : if  $u_- \leq c \leq u_+$ , then (D3.a)  $\varphi(u_+) - \varphi(c) \leq \gamma_+(u_+ - c)$  and (D3.b)  $\varphi(u_-) - \varphi(c) \leq 0$ , and if  $u_- \geq c \geq u_+$ , then (D.3c)  $\varphi(u_+) - \varphi(c) \geq \gamma_+(u_+ - c)$  and (D.3d)  $\varphi(u_-) - \varphi(c) \geq 0$ .

(D.4) (8) holds in the strong  $L^1$  sense:  $\lim_{t \downarrow 0} \int_{\mathbb{R}} |u(x, t) - u_0(x)| dx = 0$ .

**Remark 3.1.** For the full ECT model (5), we would have to replace  $u \in BV(\Pi_T)$  by the weaker condition  $u \in BV_t(\Pi_T)$ . Here  $BV_t(\Pi_T)$  is the class of functions  $W(x, t)$  with  $\partial_t W$  being a finite measure. The discontinuities in  $\gamma$  make it difficult (for (5)) to get global control of the spatial variation of  $u$ . Furthermore, it is clear from (10), (11) that if  $u$  is an entropy solution in the sense of Definition 3.1, then  $u$  is an entropy solution in the usual Kruřkov sense of  $u_t + \varphi(u)_x = 0$  for  $x < 0$  and of  $u_t + (\varphi(u) - \gamma_+ u)_x = 0$  for  $x > 0$ . Finally, (7) involves a so-called non-conservative product: a  $\delta$ -like function,  $u_x$ , is multiplied by a discontinuous function  $\gamma(x)$ . It is natural to presume that a jump condition of the following type holds across  $x = 0$ :

$$(12) \quad \varphi(u_+) - \varphi(u_-) = \bar{\gamma}(u_+ - u_-), \quad 0 = \gamma_- \leq \bar{\gamma} \leq \gamma_+.$$

In fact, when  $u_- \leq u_+$ , we can take  $c = u_-$  in (D.3a) and then  $c = u_+$  in (D.3b) to get  $0 \leq \varphi(u_+) - \varphi(u_-) \leq \gamma_+(u_+ - u_-)$ , which implies (12). Similarly, when  $u_- \geq u_+$ , we can take  $c = u_-$  in (D.3c) and then  $c = u_+$  in (D.3d) to get  $\gamma_+(u_+ - u_-) \leq \varphi(u_+) - \varphi(u_-) \leq 0$ , which again implies (12).

We are now ready to prove that entropy solutions are  $L^1$  stable and hence unique.

**Theorem 3.1** ( $L^1$  stability and uniqueness). *Let  $u$  and  $v$  be two entropy solutions in the sense of Definition 3.1 of (7)–(9) with initial data  $u_0$  and  $v_0$ , respectively. Then, for all  $t \in (0, T)$ ,  $\int_{\mathbb{R}} |u(x, t) - v(x, t)| dx \leq \int_{\mathbb{R}} |u_0(x) - v_0(x)| dx$ . In particular, there exists at most one entropy solution of (7)–(9).*

*Proof.* Using the doubling of variables technique [13], one can derive from (10) and (11) the inequality  $\int_{\mathbb{R}} |u(\cdot, t_2) - v(\cdot, t_2)| dx - \int_{\mathbb{R}} |u(\cdot, t_1) - v(\cdot, t_1)| dx \leq E$ , where  $E := \int_{t_1}^{t_2} \{ \text{sgn}(v_+ - u_+) (\varphi(v_+) - \varphi(u_+) - \gamma_+(v_+ - u_+)) - \text{sgn}(v_- - u_-) (\varphi(v_-) - \varphi(u_-)) \} dt$ . To prove the  $L^1$  contraction property, we must verify that  $E \leq 0$  by using the jump conditions. One actually shows that  $S := \text{sgn}(v_+ - u_+) (\varphi(v_+) - \gamma_+ v_+ - \varphi(u_+) + \gamma_+ u_+) - \text{sgn}(v_- - u_-) (\varphi(v_-) - \varphi(u_-)) \leq 0$  by examining all orderings of  $u_-, u_+, v_-, v_+$ , see [3] for details.  $\square$

#### 4. NUMERICAL SCHEME AND SOME PROPERTIES

We define the spatial cells  $I_j := [x_{j-1/2}, x_{j+1/2})$ ,  $j \in \mathbb{Z}$ , where  $x_k = k\Delta x$  for  $2k \in \mathbb{Z}$ . Similarly, the time interval  $(0, T)$  is discretized via  $t_n = n\Delta t$  for  $n = 0, \dots, N = \lfloor T/\Delta t \rfloor + 1$ , which results in the time strips  $I^n := [t_n, t_{n+1})$ ,  $n = 0, \dots, N - 1$ . Here  $\Delta x > 0$  and  $\Delta t > 0$  denote the discretization parameters. The CFL condition  $\lambda \max_{u \in [0, 1], x \in \mathbb{R}} |f_u(\gamma(x), u)| + \lambda \max_{x \in \mathbb{R}} \gamma^3(x) \leq 1/2$ , where  $\lambda := \Delta t / \Delta x$ , is assumed to hold. When sending  $\Delta \downarrow 0$  we will keep  $\lambda$  constant.

Let  $U_j^n$  denote the approximation to  $u(x_j, t^n)$ . Then our scheme is given by

$$(13) \quad U_j^{n+1} = U_j^n - \lambda \Delta_- h(\gamma_{j+1/2}, U_{j+1}^n, U_j^n) + \lambda \gamma_j^3 \Delta_+ U_j^n.$$

Here  $\gamma_{j+1/2} = \gamma(x_{j+1/2} -)$ , and  $\gamma_j^3 := \gamma^3(x_j -)$ . The main difference between (13) and the scheme defined [5] is the ‘sink’ term  $\lambda \gamma_j^3 \Delta_+ U_j^n$ . The use of the forward difference  $\Delta_+$  is deliberate here; we bias this difference to preserve the upwind nature of the scheme. Here we explicitly use the assumption that  $\gamma^3(x) \geq 0$ .

The numerical flux  $h(\gamma, v, u)$  appearing in (13) is the Engquist-Osher (EO henceforth) numerical flux  $h(\gamma, v, u) := \frac{1}{2}(f(\gamma, u) + f(\gamma, v)) - \frac{1}{2} \int_u^v |f_u(\gamma, w)| dw$ . We introduce  $u^\Delta(x, t) := \sum_{n=0}^N \sum_{j \in \mathbb{Z}} \chi_j^n(x, t) U_j^n$ , where  $\chi_j^n$  is the indicator for the rectangle  $I_j \times I^n$ , to define an approximate solution on all of  $\Pi_T$ .

Although the scheme is not conservative, several important properties of monotonicity are preserved. The following lemma is adapted from Lemma 3.1 of [5].

**Lemma 4.1.** *The computed solution  $U_j^n$  belongs to the interval  $[0, 1]$ . Moreover, the difference scheme (13) is monotone.*

Next we establish a fundamental time-continuity estimate.

**Lemma 4.2.** *The inequality  $\Delta x \sum_{j \in \mathbb{Z}} |U_j^{n+1} - U_j^n| \leq \Delta x \sum_{j \in \mathbb{Z}} |U_j^1 - U_j^0| \leq C \Delta t$  holds with a constant  $C$  that is independent of  $\Delta$  and  $n$ .*

The proof is similar to that of Lemma 3.2 of [5] and is omitted, see [3].

Lemmas 4.1 and 4.2 provide important stability properties of our difference scheme. We now focus on the reduced problem.

#### 5. CONVERGENCE TO AN ENTROPY SOLUTION FOR THE REDUCED PROBLEM

We can write the scheme for this reduced problem as

$$(14) \quad U_j^{n+1} = U_j^n - \lambda \Delta_- h(U_{j+1}^n, U_j^n) + \lambda \gamma_j \Delta_+ U_j^n,$$

where  $h(v, u) = \frac{1}{2}(\varphi(v) + \varphi(u)) - \frac{1}{2} \int_u^v |\varphi'(w)| dw$ . The appropriate CFL condition for our reduced problem is

$$(15) \quad \lambda \max_{u \in [0,1]} |\varphi'(u)| + \lambda \max_{x \in \mathbb{R}} \gamma(x) \leq 1/2.$$

In what follows, we utilize the incremental form of the scheme (14):

$$(16) \quad \begin{aligned} U_j^{n+1} &= U_j^n + C_{j+1/2}^n \Delta_+ U_j^n - D_{j-1/2}^n \Delta_- U_j^n, \\ C_{j+1/2}^n &= \lambda \left( \frac{\varphi(U_j^n) - h(U_{j+1}^n, U_j^n)}{\Delta_+ U_j^n} + \gamma_j \right), \quad D_{j-1/2}^n = \lambda \frac{\varphi(U_j^n) - h(U_j^n, U_{j-1}^n)}{\Delta_- U_j^n}. \end{aligned}$$

The monotonicity of  $h$ ,  $\gamma_j \geq 0$ , and (15) imply that

$$(17) \quad C_{j+1/2}^n \geq 0, \quad D_{j+1/2}^n \geq 0, \quad C_{j+1/2}^n + D_{j+1/2}^n \leq 1.$$

Lemmas 4.1 and 4.2 remain valid. Let  $V_a^b(z)$  denote the total variation of  $x \mapsto z(x)$  over  $[a, b]$ . To establish compactness, we also need a spatial variation bound:

**Lemma 5.1.** *For any interval  $[a, b]$ , and any  $t \in [0, T]$  we have a spatial variation bound of the form  $V_a^b(u^\Delta(\cdot, t)) \leq C$ , where  $C$  is independent of  $\Delta$  and  $t$  for  $t \in [0, T]$ .*

*Proof.* Due to Lemma 4.2, there is a constant  $K$  such that  $\Delta x \sum_{j \in \mathbb{Z}} \sum_{n=0}^N |U_j^{n+1} - U_j^n| \leq K$ . Fix  $r > 0$  with  $r > \Delta x$  for all mesh sizes  $\Delta x$  of interest. Let  $\mathcal{A}_0 := \mathcal{A}_0(\Delta) := \{j | x_j \in [a - r - \Delta x, a]\}$  and  $\mathcal{A}_1 := \mathcal{A}_1(\Delta) := \{j | x_j \in [b, b + r + \Delta x]\}$ , and observe that  $|\mathcal{A}_k| \Delta x \geq r$ ,  $k = 0, 1$ . It is then clear that

$$(18) \quad \Delta x \sum_{j \in \mathcal{A}_k} \sum_{n=0}^N |U_j^{n+1} - U_j^n| \leq K, \quad k = 0, 1.$$

We can choose  $j_k$  with  $j_k + k \in \mathcal{A}_k$ ,  $k = 0, 1$  such that  $\sum_{n=0}^N |U_{j_k+k}^{n+1} - U_{j_k+k}^n| = \min_{j \in \mathcal{A}_k} \sum_{n=0}^N |U_j^{n+1} - U_j^n|$  for  $k = 0, 1$ . It follows from (18) that

$$(19) \quad \sum_{n=0}^N |U_{j_k+k}^{n+1} - U_{j_k+k}^n| \leq \frac{K}{|\mathcal{A}_k| \Delta x} \leq \frac{K}{r}, \quad k = 0, 1.$$

Using the incremental form (16) and (17), we may proceed as in the proof of Harten's lemma (Lemma 2.2 of [9]) to obtain  $\sum_{j=j_0}^{j_1} |\Delta_+ U_j^{n+1}| \leq \sum_{j=j_0}^{j_1} |\Delta_+ U_j^n| + |U_{j_0}^{n+1} - U_{j_0}^n| + |U_{j_1+1}^{n+1} - U_{j_1+1}^n|$ , see [3] for details. Proceeding by induction, and then using (19), we eventually find that for  $1 \leq n \leq N$ ,  $\sum_{j=j_0}^{j_1} |\Delta_+ U_j^n| \leq \sum_{j=j_a}^{j_b} |\Delta_+ U_j^0| + 2K/r$ . The proof is completed with the observation that  $[a, b] \subseteq [x_{j_0}, x_{j_0+1}]$ , along with the assumption that  $u_0$  has bounded variation.  $\square$

**Remark 5.1.** *It is clear from (16) that we could have simply used Harten's lemma [9] in its unmodified form to conclude that the scheme is Total Variation Diminishing (TVD), thus giving a direct proof of a global spatial variation bound. We chose this more involved proof because for the complete model (5), the discontinuities in the spatially varying coefficient  $\gamma$  preclude elementary TVD type arguments like Harten's lemma. We would only have the time continuity estimate (Lemma 4.2) from which to derive a spatial variation bound, and this more local variation bound would have to suffice. Finally, note that our local BV approach could be applied to simplify the compactness proof for models similar to that of [5], see [7].*

Our spatial BV bounds carry over to the limit solution  $u$ , so that we have limits from both the left and right, denoted  $u_-(t)$ ,  $u_+(t)$  or simply  $u_-$ ,  $u_+$ , for a.e.  $t \in [0, T]$ .

We recall the notation  $a \vee b := \max\{a, b\}$ ,  $a \wedge b := \min\{a, b\}$ .

**Lemma 5.2.** *Any (subsequential) limit  $u$  of the scheme (14) satisfies the entropy conditions (10)–(D.3d).*

*Proof.* The proof of (10), (11) is standard, and is omitted. To prove (D.3a), we use a discrete entropy inequality that follows from the monotonicity property of the scheme. By means of a particular regularization of  $\gamma(x)$  and using a Lax-Wendroff-type argument, we eventually obtain the inequality  $\iint_{\Pi_T} ((u \vee c)\psi_t + (\varphi(u \vee c) - \gamma(x)v)\psi_x) dx dt - \gamma_+ c \int_0^T \psi(0, t) dt \geq 0$ . By applying a standard test function argument to this inequality, we find that for a.e.  $t \in (0, T)$ ,  $\varphi(u_-(t) \vee c) - \gamma_- c - (\varphi(u_+(t) \vee c) - \gamma_+(u_+(t) \vee c)) - \gamma_+ c \geq 0$ . Recalling that  $\gamma_- = 0$ ,  $u_- \leq c \leq u_+$ , dropping the dependence on  $t$ , and rearranging, this inequality becomes  $\varphi(u_+) - \varphi(c) \leq \gamma_+(u_+ - c)$ , and the proof of (D.3a) is complete. The proofs of (D.3b)–(D.3d) are analogous. See [3] for details.  $\square$

**Theorem 5.1** (Main Theorem). *As  $\Delta \downarrow 0$ , the approximations  $u^\Delta$  generated by (14) converge in  $L^1(\Pi_T)$  and a.e. in  $\Pi_T$  to the unique entropy solution  $u$  of (7)–(9).*

*Proof.* Recalling the proof of Lemma 5.1, we see that the constant  $C$  is independent of the interval  $[a, b]$ . Letting  $a \rightarrow -\infty$ ,  $b \rightarrow \infty$ , we obtain a uniform spatial variation bound over all of  $\mathbb{R}$ . Thus, we have an  $L^\infty$  bound (Lemma 4.1), a time continuity bound (Lemma 4.2), and a spatial variation bound (Lemma 5.1). In addition, it is a straightforward exercise, using Lemma 4.2, to derive an  $L^1(\Pi_T)$  bound for  $u^\Delta$ . Moreover, these bounds are independent of  $\Delta$ , for  $(x, t) \in \Pi_T$ . It follows from standard compactness arguments that there is a subsequential limit, converging in  $L^1(\Pi_T)$ , and a.e. in  $\Pi_T$ , which we will denote  $u$ . A proof of (D.4) is standard and is thus omitted. The proof is completed with an application of our Lemma 5.2, which guarantees that the subsequential limit  $u$  is an entropy solution. By our uniqueness result (Theorem 3.1), the entire sequence converges to  $u$ .  $\square$

Theorem 5.1 shows that there exists a unique entropy solution to the initial value problem (7)–(9), i.e., that this problem is well-posed.

**Remark 5.2.** *We have focused on the reduced model to highlight the aspects of the problem that are unique to the sink feature. By combining the definition of entropy solution and the results of this note with those of [5], one can derive a version of Theorem 5.1 that applies to the full problem. Specifically, the scheme (13) converges to the unique entropy solution of the full problem.*

## 6. NUMERICAL EXAMPLE

We consider the full ECT model (4)–(5), (8) and the flux function (1) with  $v_\infty = 6.75$ ,  $n = 5$  and  $u_{\max} = 1$ . The vessel is as shown in Figure 1 with  $x_L = -2$ ,  $x_D = -1$  and  $x_D = 1$ . We use  $\Delta x = 1/80$ ,  $\Delta t = 1/1504$ ,  $u_0 \equiv 0$ ,  $q_R = 0.6$ , and the piecewise constant parameters  $(q_L, q_D, u_F) = (0, -1, 0.7)$  for  $0 \leq t < 10$ ,  $(-0.7, -0.3, 0.7)$  for  $10 \leq t < 15$  and  $(-0.7, -0.3, 0.2)$  for  $t \geq 15$ . Figure 2 shows the numerical solution, which includes transitions between three steady states.

## REFERENCES

- [1] E. Audusse and B. Perthame, Uniqueness for a scalar conservation law with discontinuous flux via adapted entropies, *Proc. Royal Soc. Edinburgh Sect. A* **135** (2004), 253–265.
- [2] F. Bachmann and J. Vovelle, Existence and uniqueness of entropy solution of scalar conservation laws with a flux function involving discontinuous coefficients, *Comm. Partial Differential Equations* **31** (2006), 371–395.

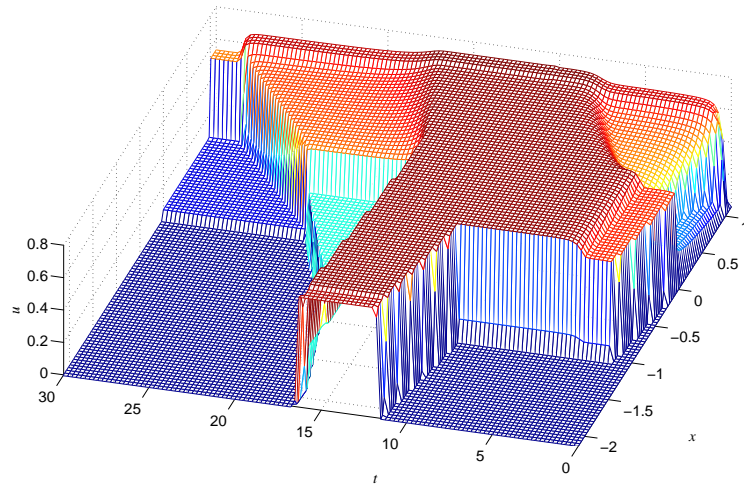


FIGURE 2. Simulation of the ECT model with piecewise constant control functions.

- [3] R. Bürger, A. García, K.H. Karlsen and J.D. Towers, On an extended clarifier-thickener model with singular source and sink terms, *Eur. J. Appl. Math.*, to appear.
- [4] R. Bürger, K.H. Karlsen, C. Klingenberg and N.H. Risebro, A front tracking approach to a model of continuous sedimentation in ideal clarifier-thickener units, *Nonlin. Anal. Real World Appl.* **4** (2003), 457–481.
- [5] R. Bürger, K.H. Karlsen, N.H. Risebro and J.D. Towers, Well-posedness in  $BV_t$  and convergence of a difference scheme for continuous sedimentation in ideal clarifier-thickener units, *Numer. Math.* **97** (2004), 25–65.
- [6] R. Bürger, K.H. Karlsen and J.D. Towers, A model of continuous sedimentation of flocculated suspensions in clarifier-thickener units, *SIAM J. Appl. Math.* **65** (2005), 882–940.
- [7] R. Bürger, K.H. Karlsen and J.D. Towers, A discontinuous viscosity scheme for conservation laws with a spatially discontinuous coefficient. In preparation.
- [8] S. Diehl, Operating charts for continuous sedimentation III: Control of step input, *J. Eng. Math.*, to appear.
- [9] A. Harten, High resolution schemes for hyperbolic conservation laws, *J. Comp. Phys.* **49** (1983), 357–393.
- [10] K.H. Karlsen, C. Klingenberg and N.H. Risebro, A relaxation scheme for conservation laws with a discontinuous coefficient, *Math. Comp.* **73** (2003), 1235–1259.
- [11] K.H. Karlsen, N.H. Risebro and J.D. Towers,  $L^1$  stability for entropy solutions of nonlinear degenerate parabolic convection-diffusion equations with discontinuous coefficients, *Skr. K. Nor. Vid. Selsk.* (2003), 49 pp.
- [12] K.H. Karlsen and J.D. Towers, Convergence of the Lax-Friedrichs scheme and stability for conservation laws with a discontinuous space-time dependent flux, *Chin. Ann. Math.* **25B** (2003), 287–318.
- [13] S.N. Kružkov, First order quasilinear equations in several independent variables, *Math. USSR Sb.* **10** (1970), 217–243.
- [14] S. Mishra, Convergence of upwind finite difference schemes for a scalar conservation law with indefinite discontinuities in the flux function, *SIAM J. Numer. Anal.* **43** (2005), 559–577.
- [15] N. Seguin and J. Vovelle, Analysis and approximation of a scalar conservation law with a flux function with discontinuous coefficients, *Math. Models Meth. Appl. Sci.* **13** (2003), 221–257.
- [16] J.D. Towers, A difference scheme for conservation laws with a discontinuous flux: The non-convex case, *SIAM J. Numer. Anal.* **39** (2001), 1197–1218.